ARMY RESEARCH LABORATORY

SOME POTENTIAL ERRORS IN SATELLITE WIND ESTIMATES USING THE GEOSTROPHIC APPROXIMATION AND THE THERMAL WIND

James Cogan

ARL-MR-36 June 1993

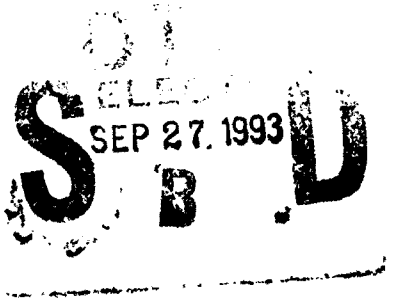

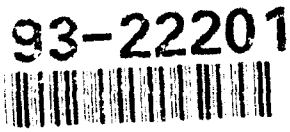

NOTICES

Disclaimers

The findings in this report are not to be construed as an official Department of the Army position, unless so designated by other authorized documents.

The citation of trade names and names of manufacturers in this report is not to be construed as official Government indorsement or approval of commercial products or services referenced herein.

Destruction Notice

When this document is no longer needed, destroy it by any method that will prevent disclosure of its contents or reconstruction of the document.

REPORT DOCUMENTATION PAGE

Form Approved
OMB No. 0704-0188

1. AGENCY USE ONLY (Leave blank)	2. REPORT DATE	3. REPORT TYPE AND DATES COVERED
	June 1993	Final

4. TITLE AND SUBTITLE

SOME POTENTIAL ERRORS IN SATELLITE WIND ESTIMATES USING THE GEOSTROPHIC APPROXIMATION AND THE THERMAL WIND

5. FUNDING NUMBERS

62784/AH71 (6.2)

6. AUTHOR(S)

James Cogan

7. PERFORMING ORGANIZATION NAME(S) AND ADDRESS(ES)

U.S. Army Research Laboratory
Battlefield Environment Directorate
ATTN: AMSRL-BE
White Sands Missile Range, NM 88002-5501

8. PERFORMING ORGANIZATION REPORT NUMBER

ARL-MR-36

9. SPONSORING/MONITORING AGENCY NAME(S) AND ADDRESS(ES)

U.S. Army Research Laboratory
2800 Powder Mill Road
Adelphi, MD 20783-1145

10. SPONSORING/MONITORING AGENCY REPORT NUMBER

11. SUPPLEMENTARY NOTES

12a. DISTRIBUTION/AVAILABILITY STATEMENT

Approved for public release; distribution unlimited.

12b. DISTRIBUTION CODE

13. ABSTRACT *(Maximum 200 words)*

Current and planned passive sensors on meteorological satellites measure radiances that are converted directly into temperature and humidity soundings. In turn, wind velocity is derived from the temperature soundings and other derived variables (for example, geopotential heights). Current operational methods involve either the geostrophic wind or the thermal wind approximation. This report presents some information and sample calculations on the types of errors that may be expected when either approximation is used to estimate the actual wind from data gathered by passive satellite sensors. The assumption is that no additional data are available (that is, only satellite sounding data from sensors of the type found on present day environmental satellites). This report does not treat the improvements that should occur when data from other sources of data (for example, radar profilers, ground-based radiometers, unmanned aerial vehicles) are combined with the satellite data.

14. SUBJECT TERMS

Satellite winds, sattelite wind errors, geostrophic wind, thermal wind

15. NUMBER OF PAGES

31

16. PRICE CODE

17. SECURITY CLASSIFICATION OF REPORT	18. SECURITY CLASSIFICATION OF THIS PAGE	19. SECURITY CLASSIFICATION OF ABSTRACT	20. LIMITATION OF ABSTRACT
Unclassified	Unclassified	Unclassified	SAR

CONTENTS

LIST OF ILLUSTRATIONS

Figure

Tables

1. INTRODUCTION

Passive satellite sounders do not directly measure wind velocity; instead they derive it indirectly from the satellite temperature profile. The temperature profile is computed from radiances (infrared or microwave) emitted by volumes of atmosphere, each defined by a horizontal resolution area, and a vertical thickness according to a weighting function centered at some pressure level. The temperature profile is used to compute geopotential heights for the several pressure levels. The height field from many soundings for each pressure level is used to compute the geostrophic wind. The geostrophic wind is an approximation to the real wind that assumes frictionless flow parallel to "straight" height contours (along a great circle), where the pressure force balances the coriolis force. An alternative method involves the shear of the geostrophic wind, commonly referred to as the "thermal wind." For a given layer, thermal wind may be derived by using the gradient of mean layer temperature or the gradient of layer thickness. Since the thermal wind is really a shear, the wind velocity at some baseline level must be measured or computed (for example, geostrophic or measured wind at 800 hPa). Figure 1 illustrates the meaning of the thermal wind through a simple example. In the example the assumption is that the geostrophic wind at 700 hPa (1 hPa = 1 mbar) has a speed and direction of 20 ms^{-1} and 240°, and at 500 hPa the values are 20 ms^{-1} and 300°. The thermal wind speed and wind direction are 20 ms^{-1} and 360°, respectively. In this case the isotherms run from north to south, with the warm air to the west. Geostrophic wind and thermal wind are defined and derived in standard texts (Haltiner and Martin 1957, Holton 1979).

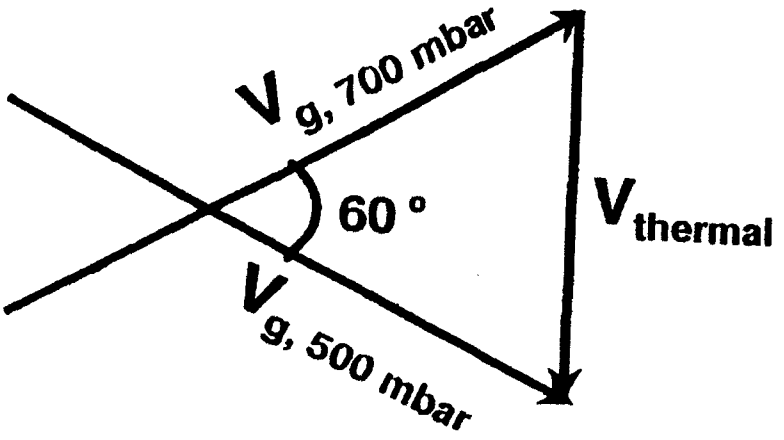

Figure 1. Illustration of the thermal wind for a layer from 700 to 500 hPa (see text).

This report presents some information and sample calculations on the types of errors that may be expected when geostrophic wind or thermal wind is used to estimate the actual wind from data gathered by passive satellite sensors. The assumption is that no additional data are available (that is, only satellite sounding data from sensors of the type found on present day environmental satellites). This report does not treat the improvements that should occur when data from other sources of data (for example, radar profilers, ground-based radiometers, unmanned aerial vehicles) are combined with the satellite data.

2. GEOSTROPHIC WIND

2.1 Basic Derivations

The equation for geostrophic wind along a constant pressure surface is given by

$$V_g = \frac{1}{f}\frac{\partial \phi}{\partial n} \tag{1}$$

where f is 2Ω sin θ (Ω sin θ is the angular velocity of the earth about the local zenith at latitude θ, and Ω is the angular velocity at the poles), n is the horizontal distance, ϕ is geopotential height, and V_g is the geostrophic wind component perpendicular to the n direction. In general, geopotential height is $\phi = \int_0^z g\,dz$ where z is height and g = gravitational acceleration. For z in meters $\phi \approx 0.98z$.

The geostrophic wind also may be computed for a constant level (height) surface where $V_g = \frac{1}{\rho f}\frac{\partial p}{\partial n}$ where $\frac{1}{\rho} = \frac{R\bar{T}_v}{\bar{p}}$ ($\bar{T}_v$ = mean virtual temperature along the distance n on the surface, $\bar{p}$ = mean pressure along that same path, and R is the gas constant for dry air). The virtual temperature accounts for moisture in the air, which having a lower density than dry air causes $T_v > T$. However, at temperatures normally found above 4 or 5 km $T \approx T_v$ and for the purposes of this report one may consider $T \approx T_v$ at satellite heights >2 *km* (generally true over land except in a moist summer or tropical atmosphere). This second form of the geostrophic wind equation can be used to check for changes caused by errors in $\bar{p}$ or $\bar{T}_v$ (or $\bar{T}$).

A similar type of "equilibrium" wind for curved parallel contours is referred to as the gradient wind. In this case, the tangential acceleration = 0. The scaler version of the equation is $V_{gr} = \frac{rf}{2}\left(-1 + \left(1 + 4\frac{V_g}{rf}\right)^{\frac{1}{2}}\right)$ where r = R tan α (R = radius of earth, α

= angular radius of the equivalent small circle for r as seen from the center of the earth, and r = radius of curvature.) The equation may be rewritten for V and V_g in knots and nautical miles, or kilometers per hour and kilometers.

$$V = 1800rf\left(-1 + \left(1 + 4\frac{V_g}{3600rf}\right)^{\frac{1}{2}}\right) \tag{2}$$

The parameter rf may be computed or extracted from standard tables to a sufficient accuracy (List 1984).

Heights of pressure levels are normally computed from the hydrostatic equation

$$z - z_o = -\frac{R\bar{T}_v}{g}\ln\left(\frac{P}{P_o}\right) \tag{3}$$

where the subscript o refers to the surface or bottom of a layer. As before, $\bar{T}$ may be substituted for $\bar{T}_v$. Here the mean value is along a vertical path for a layer of atmosphere. Computation begins at the surface or a reference p level. The height differences or layer thicknesses ($z - z_0 = \Delta z$) are "stacked" upon each other from bottom to top.

The real wind may be defined as the geostrophic wind plus an ageostrophic component. The horizontal part of this component consists of a pressure tendency term and a term involving the change in spacing of the contours (or isobars). To a sufficiently reasonable approximation (Haltner and Martin 1957), the pressure tendency $\left(\frac{\partial p}{\partial t}\right)$ term is given by

$$(V - V_g)_t \approx \frac{1}{\rho f^2}\frac{\partial\left(\frac{\partial p}{\partial t}\right)}{\partial s} \approx -\frac{1}{\rho f^2}\frac{\Delta}{\Delta s}\left(\frac{\partial p}{\partial t}\right) \tag{4}$$

where s consists of normal and tangential distances. The term for the change in contour spacing may be found by $(V - V_g)_s \approx \frac{V}{f}\frac{\partial V_g}{\partial s}$ where V is the real wind. To a fairly reasonable approximation, V on the right side may be approximated by V_g, the mean value along the distance s (in this case along a path equidistant from neighboring contours).

$$(V-V_g)_g \approx \frac{\overline{V_g}}{f}\left(\frac{\Delta V_g}{\Delta s}\right) \tag{5}$$

One may compute values that roughly estimate "typical" magnitudes of the possible errors in wind caused by the geostrophic approximation and errors in the geostrophic wind caused by errors in input values (for example, mean layer temperature). As a first step, wind speed only is considered.

2.2 Errors In V_g Caused By Mean Profile Temperature Error

The geostrophic wind for contours at 100 geopotential meters (gpm) in units of knots (List 1984) may be stated as $V_g \approx \frac{0.01712}{\Delta n}$ where Δn is in degrees of latitude. At 45° latitude and a contour interval of 30 gpm, and Δn expressed in kilometers,

$$V_g \approx \frac{5.701 \times 10^3}{\Delta n} \text{ in kn or } V_g \approx \frac{2.9387 \times 10^3}{\Delta n} \text{ in } ms^{-1} \tag{6}$$

For other contour intervals multiply by the ratio of "new interval"/30 gpm. For a typical midlatitude atmosphere (Jursa 1985), for the surface (assume at 1000 hPa) to 500 hPa layer, the possible error can be computed from net temperature profile error by using equations (3) and (6). The mean layer temperature for the April atmosphere at 45°N (Jursa 1985) is used to compute the height of the 500 hPa level.

$$\Delta z = \frac{-287\ K^{-1}m^2s^{-2}(265\ K)}{9.81\ ms^{-2}}(-0.693) = 5373.6\ m \approx 5266.1\ gpm$$

Values are computed for differences of $\overline{T}$ of 1 and 2 K, or $\overline{T}$ = 264 and 263 K.

$$\Delta z_{264} = 5353.3\ m \approx 5246.2\ gpm$$

$$\Delta z_{263} = 5333.1\ m \approx 5226.4\ gpm$$

For the case of a difference over the 1000 to 700 hPa layer for the same atmosphere,

$$\Delta z_{268} = \frac{-287\ K^{-1}m^2s^{-2}}{9.81\ ms^{-2}}(268\ K)(-0.356675) = 2797.0\ m \approx 2741.1\ gpm$$

$$\Delta z_{267} = 2786.6\ m \approx 2730.9\ gpm$$

$$\Delta z_{266} = 2776.1\ m \approx 2720.6\ gpm$$

Similar computations may be made for other layers or sublayers, for example, in table 1. We now assume a "true" $\Delta\phi$ of 30 gpm between soundings 200 km apart. The differences in $\bar{T}$ errors between the soundings are assumed to be 1 and 2 K (for example, the first s ınding has a $\bar{T}$ error of 2 K, and the second has an error of 3 K, for a difference in error of 1 K).

TABLE 1. DIFFERENCES IN GPM COMPUTED FOR THE LISTED LAYERS FOR THE LISTED DIFFERENCES IN $\bar{T}$ ERROR BETWEEN TWO SOUNDINGS 200 KM APART.

$\bar{T}$ Difference	Layer (hPa)				
(K)	1000-900	1000-800	1000-700	1000-800	1000-500
0	0	0	0	0	0
1	3.0	6.4	10.2	14.7	19.9
2	6.1	12.8	20.5	29.3	39.7

Equation (6) can be used to compute the V_g values for the "measured" difference (30 gpm) over 200 km, and V_g arising from the two $\bar{T}$ error differences (1 and 2 K), for both the entire 1000 to 500 hPa layer and the several sublayers. Table 1 shows the gpm differences and table 2 shows values of V_g.

TABLE 2. VALUE OF V_g IN ms^{-1} COMPUTED FOR THE LISTED LAYERS AND DIFFERENCES IN $\bar{T}$ ERROR BETWEEN TWO SOUNDINGS 200 KM APART. $\Delta\phi$ DIFFERENCES WERE ADDED TO THE "MEASURED" 30 GPM TO OBTAIN THE VALUES SHOWN.

$\bar{T}$ Difference	Layer (hPa)				
(K)	1000-900	1000-800	1000-700	1000-800	1000-500
0	14.7	14.7	14.7	14.7	14.7
1	16.2	17.8	19.7	21.9	24.4
2	17.7	21.0	24.7	29.0	34.1

Table 2 shows that the V_g differences are about 9.7, 5.0, and 1.5 ms^{-1} respectively for the layer and, for example, the 1000 to 700 hPa and 1000 to 900 hPa sublayers for a $\bar{T}$ error difference of 1 K. For a 2-K difference, the V_g differences are about 19.4, 10.0, and 3.0 ms^{-1}, respectively.

These differences in V_g are not small and may even result in a 180-degree change in direction (for example, subtracting 39.7 gpm from 30 gpm gives -9.7 ms^{-1} (reversed direction of the gradient) resulting in a small V_g in the opposite direction).

2.3 Errors Caused By Curved Flow

One may compute the difference in wind speed caused by the flow being curved instead of straight (along a great circle). For this comparison, the gradient wind for moderate geostrophic winds (15 and 30 ms^{-1}) is computed. From tables in List (1984) an rf parameter of 0.062 at a latitude of 45° is obtained for a radius of curvature (r) of about 600 nm (≈ 1110 km). For V_g = 15 ms^{-1},

$$V = 111.6 sh^{-1} nms^{-1} \left(-1 + \left(1 + \frac{4(29.1 nmh^{-1})}{3600 sh^{-1} 0.062 nms^{-1}} \right)^{\frac{1}{2}} \right) = 26.1 \; kn \approx 13.5 \; ms^{-1} \; .$$

Also, for V_g = 30 ms^{-1},

$$V = 47.9 \; kn \approx 24.7 \; ms^{-1}$$

The two differences $(V - V_g)$ computed above are 1.5 and 5.3 ms^{-1}.

2.4 Errors Caused by Mean Temperature Error

Another possible cause of error is an incorrect value of $\bar{T}$ but no difference in $\bar{T}$ error between the two soundings (same $\bar{T}$ error at both locations). The constant level surface version of equation (1) is used; that is, $V_g \approx \frac{R\bar{T}}{f\bar{p}} \frac{\Delta p}{\Delta n}$, where the assumption is that

$$\Delta p = 20 \; mbar, \; \Delta n = 1000 \; km, \; \bar{p} = 700 \; mbar, \; lat = 45°$$

For $\bar{T}$ = 270 K,

$$V_g = \frac{(287 \; K^{-1} m^2 s^{-2}) \; 270 \; K}{1.03(10^{-4}) s^{-1} \; 700 \; mbar} \left(\frac{20 \; mbar}{10^6 \; m} \right) = 21.5 \; ms^{-1} \quad ,$$

and for $\overline{T}$ = 267 K,

$$V_g = 21.3\ ms^{-1} \quad .$$

The difference in these moderate values of V_g is about 0.2 ms^{-1}. The likely error of a few tenths of a meter per second for moderate V_g is small relative to the other possible errors.

2.5 Errors From Ageostrophic Deviations

A significant potential source of error arises from not considering certain deviations from the geostrophic wind, which may be roughly approximated by the horizontal ageostrophic wind components. Equation (4) may be used to approximate the ageostrophic component arising from the pressure tendency.

Here a pressure tendency normal to the wind of -1 hPa over 1 h near 45° latitude is considered. One hPa = 10 $kg\ m^{-1}s^{-2}$ and the air density (ρ) = 1 $kg\ m^{-3}$.

$$(V - V_g)_t \approx \frac{-1}{1\ kg\ m^{-3}(1.03\ s^{-1})^2}\left(\frac{1}{2\ m}\right)\left(\frac{-10\ kg\ m^{-1}s^{-2}}{3600\ s}\right) \approx 1.3\ ms^{-1}$$

If the tangential component was the same size, the rough magnitude of the total pressure tendency term would be about 1.7 ms^{-1}.

Equation (5) expresses the ageostrophic component arising from a change in the spacing of contours on a constant pressure surface (or isobars on a constant height surface). A change of geostrophic wind of 2 ms^{-1} over a distance of 200 km is not unreasonable. For geostrophic wind speeds of 15 ms^{-1} and 30 ms^{-1}, at 45° latitude,

$$(V - V_g)_s \approx \frac{15\ ms^{-1}}{1.03(10^{-4})s^{-1}}\left(\frac{2\ ms^{-1}}{2(10^5)m}\right) \approx 1.5\ ms^{-1}$$

and $(V - V_g)_s \approx 2.9\ ms^{-1}$

Higher values of V_g or ΔV_g can occur, leading to higher values of this "contour spacing" component. When both components are combined, the ageostrophic part of the "real" horizontal wind may exceed 5 ms^{-1} (or < 1 ms^{-1} if the two terms tend to cancel or V_g is small).

2.6 Apparent Error From Direction Deviations

So far the error caused by incorrect orientation of the gradient has not been explicitly considered. Jedlovec (1985) reported on differences between gradients derived from data of the visible infrared spin scan radiometer (VISSR) atmospheric sounder (VAS) carried on the geostationary operational environmental satellite (GOES) and those computed using data from a special dense net of rawinsondes (50-km spacing). The differences ranged from a few degrees (almost parallel) to about 90° (nearly perpendicular). In the absence of other factors, an error in direction of the gradient (or contours) of around 30° could lead to a difference in V_g along the expected wind direction of about 2.0 and 4.0 ms^{-1} for V_g values of 15 and 30 ms^{-1}, respectively. A realistic high deviation in gradient near 45° could produce V_g differences of about 4.4 and 8.8 ms^{-1} for the aforementioned V_g values. While even good quality data from rawinsondes may contain wind velocity errors, the deviations in direction reported by Jedlovec (1985) may reflect real differences from the true direction of the gradient (or contours).

2.7 Net Error Values

Table 3 lists some of the potential causes of error in satellite-derived estimates of wind speed that use the geostrophic wind, along with possible magnitudes of those errors. A moderate wind speed is assumed (10 to 30 ms^{-1}).

TABLE 3. POSSIBLE MAGNITUDES OF ERROR IN WIND SPEED ARISING FROM LISTED CAUSES FOR SATELLITE-DERIVED GEOSTROPHIC WINDS.

	Cause	Resultant Wind Speed Error (ms^{-1})
1	Incorrect $\bar{T}$	0.1 to 0.4
2	Gradient instead of Geostrophic Flow	1 to 5
3	Computed contour gradient incorrect (varying error in T sounding)*	5 to 20
4	Ageostrophic component Pressure tendency Contour spacing change	 0.5 to 2 1 to 5
5	Incorrect direction of gradient (height or pressure)	Near 0 to 10 (Component in expected direction of wind)

*For the T sounding error (item 3) a layer of at least 300 hPa was assumed (for example, near sea level surface to about 3 km AGL, the region of largest satellite temperature error over land).

These values may tend to augment or cancel one another. For example, items 3 and 4 may result in errors of over 20 ms^{-1} or only 1 or 2 ms^{-1}. Miers et al. (1992) and their references report satellite geostrophic wind errors from ± 4 to ± 14 ms^{-1}, generally compared with wind speeds measured by rawinsondes. Rawinsonde data also may have errors, ranging from < 1 ms^{-1} for high quality equipment to > 2.5 ms^{-1} for older (now mostly obsolete) equipment (Fisher et al. 1987). Reasonable "middle of the road" errors (1 to 4 of table 3) from this analysis may lead to a "total error of about 15 to 20 ms^{-1} where the individual errors sum together or perhaps only 2 or 3 ms^{-1} where they largely cancel.

Deviations in direction of the gradient or contours from the actual direction (Miers et al. 1992, Jedlovec 1985) could result in apparent errors of up to 10 ms^{-1}. This "error" would be important for computing the wind speed for a specified direction. An example would be the cross or along trajectory wind speed for an artillery application. The apparent error (but a real component error) could either increase or decrease the "true" error. For example, an error in wind speed of 10 ms^{-1} combined with a deviation in gradient direction could result in a down range error of approximately 15 or 5 ms^{-1}.

The net errors shown in table 3 represent a range of "typical" values for moderate wind speeds (10 to 30 ms^{-1}). However, the reader may compute other values of potential errors for greater or lesser wind speeds, as well as for other parameters (for example, different radii of curvature, or differences in $\bar{T}$ error less than 0.5 K or greater than 2 K). The reader may elect to calculate new potential errors for one or more of the causes of table 3 to arrive at additional net error values. Appendix A contains a selection of tables from List (1984) that should suffice, along with the equations presented herein, for nearly all additional calculated errors.

3. THERMAL WIND

3.1 Basic Derivations

A number of texts provide information on formulations of the thermal wind (Haltiner and Martin 1957, Holton 1979). The form derived in Holton (1979) is used here. Given the horizontal components of the geostrophic wind in geopotential form,

$$u_g = -\frac{1}{f}\frac{\partial \phi}{\partial y} \quad \text{and} \quad v_g = \frac{1}{f}\frac{\partial \phi}{\partial x} \tag{7}$$

and

$$\frac{\partial \phi}{\partial p} = -\frac{1}{\rho} = \frac{RT}{p} \tag{8}$$

When equation (7) is differentiated with respect to p and equation (8) is applied, the results are

$$p\frac{\partial v_g}{\partial g} = \frac{\partial v_g}{\partial \ln p} = -\frac{R}{f}\left(\frac{\partial T}{\partial x}\right)_p$$

$$p\frac{\partial u_g}{\partial p} = \frac{\partial u_g}{\partial \ln p} = \frac{R}{f}\left(\frac{\partial T}{\partial y}\right)_p$$

or in vector form $\frac{\partial \underline{V}_g}{\partial \ln p} = -\frac{R}{f}\,\underline{k} \times (\nabla T)_p$

and $\underline{V}_T = \underline{V}_g(p_1) - \underline{V}_g(p_o) = -\frac{R}{f}\int_{p_o}^{p_1}(\underline{k} \times \nabla T)\,d\ln p$

where T = temperature, p = pressure, ρ = density, R = gas constant for dry air, ϕ = geopotential, and $\underline{V}_g$ = geostrophic wind. f is the coriolis parameter (= 2 $\Omega \sin\theta$ where Ω is the angular velocity of the earth at the poles and θ is latitude). In component form

$$u_T = -\frac{R}{f}\left(\frac{\partial \bar{T}}{\partial y}\right)_p \ln\left(\frac{p_o}{p_1}\right) \tag{9}$$

$$v_T = \frac{R}{f}\left(\frac{\partial \bar{T}}{\partial x}\right)_p \ln\left(\frac{p_o}{p_1}\right) \tag{10}$$

where $u_T = u_g(p_1) - u_g(p_o)$ and $v_T = v_g(p_1) - v_g(p_o)$ are the thermal wind components defined as the differences in the geostrophic components for the upper p surface, denoted with subscript 1, and the lower p surface, denoted by subscript o. $\bar{T}$ is the mean temperature for the layer from p_o to p_1, and x and y are distances in the east-west and north-south directions, respectively. An alternative method is to use the geopotential form, or the equivalent "height" form.

$$u_T = -\frac{1}{f}\frac{\partial(\phi_1 - \phi_o)}{\partial y} = -\frac{g}{f}\frac{\partial(z_1 - z_o)}{\partial y}$$

$$v_T = \frac{1}{f}\frac{\partial(\phi_1 - \phi_o)}{\partial x} = \frac{g}{f}\frac{\partial(z_1 - z_o)}{\partial x}$$

Since this paper is concerned with errors in satellite temperature soundings, equations (9) and (10) will be used.

3.2 Errors From Incorrect Mean Temperatures

Equations (9) and (10) may be approximated in finite difference form to a sufficient accuracy.

$$u_T \approx - \frac{R}{f}\left(\frac{\Delta \bar{T}}{\Delta y}\right)_p \ln\left(\frac{p_o}{p_1}\right)$$

$$v_T \approx \frac{R}{f}\left(\frac{\Delta \bar{T}}{\Delta x}\right)_p \ln\left(\frac{p_o}{p_1}\right)$$

Taking differences in errors in $\bar{T}$ between soundings 200 km apart of 0.5, 1, and 2 K, one can compute potential discrepancies in thermal wind for given layers of atmosphere. The 700 to 300 hPa layer will be considered as a whole and subdivided into 100 hPa sublayers. Isotherms orientation will be assumed to be NE-SW (45°) and latitude to be 43°. For the entire layer, for a 2-K error in $\bar{T}$

$$u_T \approx - \frac{287\ K^{-1}m^2s^{-2}}{10^{-4}\ s^{-1}}\left(\frac{1.414\ K}{141.4\ (10^3)m}\right)(0.8473) \approx - 28.7(0.8473)$$

$$\approx - 24.3\ ms^{-1}$$

$$v_T \approx 24.3\ ms^{-1}$$

The magnitude (wind speed) from the standard formula is

$$V_T = \left(u_T^2 + v_T^2\right)^{\frac{1}{2}} = 34.4\ ms^{-1}$$

For a 1-K error in $\bar{T}$,

$$u_T \approx 12.15\ ms^{-1}$$

$$v_T \approx 12.15\ ms^{-1}$$

$$V_T \approx 17.2\ ms^{-1}$$

For 0.5-K error in $\bar{T}$,

$$V_T \approx 8.6\ ms^{-1}$$

Table 4 shows the values for individual sublayers (I) and the cumulative error (sum of errors from lowest to given layer, C). Slight differences between last cumulative values and values for entire 700 to 300 hPa layer appear because of round off of table values.

TABLE 4. THERMAL WIND VALUES (ms^{-1}) FOR LISTED LAYERS AND DIFFERENCES IN ERRORS IN MEAN TEMPERATURE ($\bar{T}$) BETWEEN SOUNDINGS 200 KM APART.

$\bar{T}$ Difference	Layers (hPa)							
	700-600		600-500		500-400		400-300	
	I	C	I	C	I	C	I	C
0.5	1.6	1.6	1.8	3.4	2.3	5.7	2.9	8.6
1	3.1	3.1	3.7	6.8	4.5	11.3	5.8	17.1
2	6.3	6.3	7.4	13.7	9.1	22.8	11.7	34.5

3.3 Net Potential Error

The results shown in table 4 do not include possible errors in the baseline wind field (for example, wind at 700 hPa), errors arising from not considering curvature, and ageostrophic components. Use of measured wind as the baseline value will reduce the total possible error. However, since the thermal wind itself makes use of the geostropic approximation, the other sources of error may have an increasingly greater effect as height from the baseline level increases.

As a first estimate of potential errors, one can use the values of table 3, with the range of values from table 4 replacing item 3 (varying error in T sounding causing incorrect contour gradient). Table 5 repeats part of table 3 along with new results from table 4 for a 700 to 300 hPa layer. The values of item 1 of table 5 would be smaller for thinner layers (for example, a range of $<1\ ms^{-1}$ to around 12 ms^{-1} for differences in $\bar{T}$ error of a few tenths of a degree to about 2 K for a 100 hPa thick layer).

These errors may tend to augment or cancel one another. For example, items 1 and 3 may result in errors of over 35 ms^{-1}, or only 1 or 2 ms^{-1}. For thinner layers (for example, 700 to 500 hPa) the value of item 1 would be much smaller (table 4), reducing

the overall potential error. However, the numbers in table 2 assume a "perfect" measured wind velocity at 700 hPa. The wind speed error of measured wind (rawinsonde or radar profiler) is likely to have a value near 1 to 2 ms^{-1} (Miers et al. 1992, Fisher et al. 1987). This error also may augment or diminish the "thermal wind" error. Some rough idea of potential error may be obtained by assuming "middle of the road" errors from table 5 (items 1 to 3). The potential total error may reach values over 25 ms^{-1} where the individual errors sum together, or perhaps less than 10 ms^{-1} where they largely cancel.

TABLE 5. POTENTIAL MAGNITUDES OF ERROR IN THERMAL WIND GIVEN POSSIBLE DIFFERENCES IN $\overline{T}$ ERROR BETWEEN SOUNDINGS 200 KM APART.*

	Cause	Potential Wind Speed Error (ms^{-1})
1	$\overline{T}$ gradient of layer (700-300 hPa) incorrect	5 to 35
2	Gradient instead of Geostrophic (curved flow)	1 to 5
3	Ageostrophic component Pressure tendency Contour spacing change	 0.5 to 2 1 to 5
4	Incorrect direction of temperature gradient	Near 0 to 10

*The assumption is that the difference in $\overline{T}$ error does not exceed 2 K for the 700 to 300 hPa layer. Baseline wind measured at 700 hPa.

Deviations in the temperature or height gradient from the actual direction (Miers et al. 1992, Jedlovec 1985) could result in apparent errors (but a real component error) of up to 10 ms^{-1} in geostrophic wind. These same deviations could cause errors in estimates of thermal wind of about the same size for thicker layers (for example, 700 to 300 hPa). Since thinner layers (for example, 700 to 600 hPa) normally would have smaller thermal wind values, the error from deviations from the true gradient direction would be smaller, perhaps less than 3 ms^{-1}. If a measured baseline wind was not available, the error could be considerably larger. For example, for a 700 to 300 mbar layer use of the geostrophic wind as the baseline wind could lead to errors of over 40 ms^{-1} if the net thermal wind error and the error in the baseline geostrophic wind tended to sum together.

4. CONCLUSION

Errors in satellite estimates of the real wind that use the geostrophic approximation or thermal wind may reach significant values. Net differences between the actual and geostrophic wind from a few to over 20 ms^{-1} are possible, with reasonable middle values of 10 or 12 ms^{-1}. The apparent wind speed error caused by differences in orientation of the geopotential height gradient may increase (or decrease) the component of the geostrophic wind in a specific direction, resulting in an augmentation or reduction in the effect of the other "real" errors. This effect may be especially important for artillery or aviation.

Net differences between the real wind and that derived from the thermal wind may range from a few to over 30 ms^{-1} for thick layers (for example, 700 to 300 hPa), with reasonable middle values around 15 to 18 ms^{-1}. For a thin layer of approximately 100 hPa thickness, the errors may range from 1 to over 10 ms^{-1} with reasonable middle values near 3 to 6 ms^{-1}. The apparent wind speed error caused by differences in temperature gradient orientation may increase (or decrease) the component of the estimated wind in a specific direction. As with the geostrophic wind, this apparent error may augment or reduce the effect of the other "real" errors.

The potential errors described in this report may occur when satellite data are used alone, without any additional data to "tie" down the appropriate satellite values. Some improvement should be possible through the use of new sources of data (Miers et al. 1992) such as radar wind profilers and accompanying radio acoustic sounding system (RASS), ground-based radiometers, and sensors on unmanned aerial vehicles, combined with processing techniques currently under development. In addition, new satellite sensors will eliminate many of the difficulties associated with current instruments. For example, new active sensors planned for early in the next century (for example, the laser atmospheric wind sounder) will measure wind velocity directly for cloud-free lines of sight, and new passive sounders (for example, atmospheric infrared sounder) will improve temperature profiles. In the interim the combination of additional sources of data, new processing techniques, and satellite sensors coming on line by the end of the 1990's (for example, special sensor microwave imager/sounder on Defense Meteorological Satellite Program satellites, and the advanced microwave sounding unit-A on National Oceanic and Atmospheric Administration satellites) may provide the best solution. Descriptions of these sensors may be found in NASA (1991), Patel (1992), and Swadley and Chandler (1992).

REFERENCES

Fisher, E., F. Brousaides, E. Keppel, F. J. Schmidlin, H. Herring, and D. Tolzene, 1987, Meteorological Data Error Estimates, Document 353-87, Meteorology Group, Range Commander's Council, White Sands Missile Range, NM.

Haltiner, G., and F. Martin, 1957, Dynamical and Physical Met, McGraw-Hill Book Company, NY.

Holton, J.R., 1979, An Introduction to Dynamic Meteorology, 2nd Edition, Academic Press, New York, NY.

Jedlovec, G., 1985, "An Evaluation and Comparison of Vertical Profile Data from the VISSR Atmospheric Sounder (VAS)," J Adams Ocean Tech, 2:559-581.

Jursa, A. S. (Ed), 1985, Handbook of Geophysics and the Space Environment, Air Force Geophysics Laboratory, Hanscom AFB, MA.

List, R. (Ed), 1984, Smithsonian Met Tables, Smithsonian Institute Press, Washington, DC.

Miers, B., J. Cogan, and R. Szymber, 1992, Review of Selected Remote Sensor Measurements of Temperature, Wind, and Moisture, and Comparison to Rawinsonde Measurements, TR-0315, U.S. Army Research Laboratory, White Sands Missile Range, NM.

National Aeronautics and Space Administration (NASA), 1991, EOS Reference Handbook, Goddard Space Flight Center, Greenbelt, MD.

Patel, P. K., 1992, "Advanced Microwave Sounding Unit-A," Preprints of the Sixth Conference on Satellite Meteorology and Oceanography, American Meteorological Society, Atlanta, GA, 462-465.

Swadley, S. D., and J. Chandler, 1992, "The Defense Meteorological Satellite Program's Special Sensor Microwave Imager/Sounder (SSMIS): Hardware and Retrieval Algorithms," Preprints of the Sixth Conference on Satellite Meteorology and Oceanography, American Meteorological Society, Atlanta, GA, 457-461.

APPENDIX A. TABLES FOR CALCULATING GEOSTROPHIC AND GRADIENT WINDS

This appendix presents a series of tables from List that may be used as an aid in calculating geostrophic and gradient winds. Accompanying explanations are included. For further details see List (1984),[1] Haltiner and Martin (1957),[2] and Holton (1979).[3]

[1]G. Haltiner and F. Martin, 1957, Dynamical and Physical Met, McGraw-Hill Book Company, NY.

[2]J. R. Holton, 1979, An Introduction to Dynamic Meteorology, 2nd Edition, Academic Press, New York, NY.

[3]R. List (Ed), 1984, Smithsonian Met Tables, Smithsonian Institute Press, Washington, DC.

TABLE 37

GEOSTROPHIC WIND, CONSTANT PRESSURE SURFACE

100 geopotential meter contours

The scalar equation for the geostrophic wind on a constant pressure surface is

$$V_s = \frac{1}{f}\frac{\partial \Phi}{\partial n}$$

where Φ is the geopotential in a constant-pressure surface, n is distance measured in the horizontal direction, f is the coriolis parameter, and V_s is the component of the geostrophic wind normal to the direction in which n is measured.

On a constant pressure surface with contours drawn for intervals of 100 geopotential meters (gpm.) this reduces to

$$V_s(\text{knots}) = \frac{0.017120}{f\Delta n}$$

(continued on next page)

Contour spacing				Latitude							
Degrees of Latitude	Kilometers	Statute miles	Nautical miles	10° knots	15° knots	20° knots	25° knots	30° knots	35° knots	40° knots	45° knots
1.0	111	69	60	676.0	453.5	343.2	277.8	234.8	204.7	182.6	166.0
1.1	122	76	66	614.6	412.3	312.0	252.5	213.4	186.1	166.0	150.9
1.2	133	83	72	563.3	378.0	286.0	231.5	195.6	170.5	152.2	138.3
1.3	145	90	78	520.0	348.9	264.0	213.7	180.6	157.4	140.5	127.7
1.4	156	97	84	482.9	324.0	245.2	198.4	167.7	146.2	130.4	118.6
1.5	167	104	90	450.7	302.4	228.8	185.2	156.5	136.4	121.7	110.7
1.6	178	111	96	422.5	283.5	214.5	173.6	146.7	127.9	114.1	103.8
1.7	189	117	102	397.7	266.8	201.9	163.4	138.1	120.4	107.4	97.7
1.8	200	124	108	375.6	252.0	190.7	154.3	130.4	113.7	101.5	92.2
1.9	211	131	114	355.8	238.7	180.6	146.2	123.6	107.7	96.1	87.4
2.0	222	138	120	338.0	226.8	171.6	138.9	117.4	102.3	91.3	83.0
2.1	234	145	126	321.9	216.0	163.4	132.3	111.8	97.5	87.0	79.1
2.2	245	152	132	307.3	206.2	156.0	126.3	106.7	93.0	83.0	75.5
2.3	256	159	138	293.9	197.2	149.2	120.8	102.1	89.0	79.4	72.2
2.4	267	166	144	281.7	189.0	143.0	115.7	97.8	85.3	76.1	69.2
2.5	278	173	150	270.4	181.4	137.3	111.1	93.9	81.9	73.0	66.4
2.6	289	180	156	260.0	174.4	132.0	106.8	90.3	78.7	70.2	63.9
2.7	300	187	162	250.4	168.0	127.1	102.9	87.0	75.8	67.6	61.5
2.8	311	193	168	241.4	162.0	122.6	99.2	83.8	73.1	65.2	59.3
2.9	322	200	174	233.1	156.4	118.4	95.8	81.0	70.6	63.0	57.2
3.0	334	207	180	225.3	151.2	114.4	92.6	78.3	68.2	60.9	55.3
3.2	356	221	192	211.3	141.7	107.3	86.8	73.4	64.0	57.1	51.9
3.4	378	235	204	198.8	133.4	100.9	81.7	69.1	60.2	53.7	48.8
3.6	400	249	216	187.3	125.0	95.3	77.2	65.2	56.8	50.7	46.1
3.8	423	263	228	177.9	119.4	90.3	73.1	61.8	53.9	48.1	43.7
4.0	445	276	240	169.0	113.4	85.8	69.4	58.7	51.2	45.7	41.5
4.2	467	290	252	161.0	108.0	81.7	66.1	55.9	48.7	43.5	39.5
4.4	489	304	264	153.6	103.1	78.0	63.1	53.4	46.5	41.5	37.7
4.6	511	318	276	147.0	98.6	74.6	60.4	51.0	44.5	39.7	36.1
4.8	534	332	288	140.8	94.5	71.5	57.9	48.9	42.6	38.0	34.6
5.0	556	345	300	135.2	90.7	68.6	55.6	47.0	40.9	36.5	33.2
5.5	612	380	330	122.9	82.5	62.4	50.5	42.7	37.2	33.2	30.2
6.0	667	415	360	112.7	75.6	57.2	46.3	39.1	34.1	30.4	27.7
6.5	723	449	390	104.0	69.8	52.8	42.7	36.1	31.5	28.1	25.5
7.0	778	484	420	96.6	64.8	49.0	39.7	33.5	29.2	26.1	23.7
8.0	890	553	480	84.3	56.7	42.9	34.7	29.3	25.6	22.8	20.8
9.0	1001	622	540	75.1	50.4	38.1	30.9	26.1	22.7	20.3	18.4
10.0	1112	691	600	67.6	45.4	34.3	27.8	23.5	20.5	18.3	16.6

(To convert knots to other measures of speed see Table 35.)

(continued)

TABLE 37 (CONCLUDED)

GEOSTROPHIC WIND, CONSTANT PRESSURE SURFACE

100 geopotential meter contours

where Δn is the contour spacing measured in degrees of latitude (i.e., one unit of Δn has the length of one degree of latitude at the place for which the contour spacing is measured). Table 37 gives values of V, in knots as a function of Δn and latitude with auxiliary columns giving equivalents of Δn in kilometers, statute miles, and nautical miles. If the latter are measured by a map scale true at some other latitude the value should be corrected to the latitude at which the measurements are taken (see Table 165).

Since the geostrophic wind is inversely proportional to the contour spacing and directly proportional to the contour interval ($\Delta\Phi$ gpm.), values of V, for 1/10 of the indicated spacing may be found by multiplying the tabular values by 10, etc., and for contour intervals that are multiples or submultiples of 100 gpm. by multiplying the tabular values by $\Delta\Phi/100$ (e.g., for 200 gpm. contours multiply by 2, for 50 gpm. contours multiply by ½, etc.).

Contour spacing				Latitude							
Degrees of Latitude	Kilometers	Statute miles	Nautical miles	50° knots	55° knots	60° knots	63° knots	70° knots	73° knots	80° knots	85° knots
1.0	111	69	60	133.2	143.3	135.5	129.5	124.9	121.5	119.2	117.8
1.1	122	76	66	139.3	130.3	123.2	117.7	113.6	110.5	108.4	107.1
1.2	133	83	72	127.7	119.4	113.0	107.9	104.1	101.3	99.3	98.2
1.3	145	90	78	117.9	110.2	104.3	99.6	96.1	93.5	91.7	90.6
1.4	156	97	84	109.3	102.4	96.8	92.3	89.2	86.8	85.1	84.2
1.5	167	104	90	102.2	95.5	90.4	86.3	83.3	81.0	79.3	78.6
1.6	178	111	96	95.3	89.6	84.7	81.0	78.1	76.0	74.3	73.5
1.7	189	117	102	90.1	84.3	79.7	76.2	73.5	71.5	70.1	69.3
1.8	200	124	108	85.1	79.6	75.3	72.0	69.4	67.5	66.2	65.5
1.9	211	131	114	80.7	75.4	71.3	68.2	65.7	64.0	62.7	62.0
2.0	222	138	120	76.6	71.7	67.8	64.8	62.5	60.8	59.6	58.9
2.1	234	145	126	73.0	68.2	64.5	61.7	59.5	57.9	56.8	56.1
2.2	245	152	132	69.7	65.1	61.6	58.9	56.8	55.2	54.2	53.6
2.3	256	159	138	66.6	62.3	58.9	56.3	54.3	52.8	51.8	51.2
2.4	267	166	144	63.8	59.7	56.5	54.0	52.1	50.6	49.7	49.1
2.5	278	173	150	61.3	57.3	54.2	51.8	50.0	48.6	47.7	47.1
2.6	289	180	156	58.9	55.1	52.1	49.8	48.0	46.7	45.8	45.3
2.7	300	187	162	56.8	53.1	50.2	48.0	46.3	45.0	44.1	43.6
2.8	311	193	168	54.7	51.2	48.4	46.3	44.6	43.4	42.6	42.1
2.9	322	200	174	52.8	49.4	46.7	44.7	43.1	41.9	41.1	40.6
3.0	334	207	180	51.1	47.8	45.2	43.2	41.6	40.5	39.7	39.3
3.2	356	221	192	47.9	44.8	42.4	40.5	39.0	38.0	37.2	36.8
3.4	378	235	204	45.1	42.1	39.9	38.1	36.7	35.7	35.1	34.7
3.6	400	249	216	42.5	39.8	37.7	36.0	34.7	33.8	33.1	32.7
3.8	423	263	228	40.3	37.7	35.7	34.1	32.9	32.0	31.4	31.0
4.0	445	276	240	38.3	35.8	33.9	32.4	31.2	30.4	29.8	29.5
4.2	467	290	252	36.5	34.1	32.3	30.8	29.7	28.9	28.4	28.1
4.4	489	304	264	34.8	32.5	30.8	29.4	28.4	27.6	27.1	26.8
4.6	511	318	276	33.3	31.2	29.5	28.2	27.2	26.4	25.9	25.6
4.8	534	332	288	31.9	29.9	28.2	27.0	26.0	25.3	24.8	24.5
5.0	556	345	300	30.6	28.7	27.1	25.9	25.0	24.3	23.8	23.6
5.5	612	380	330	27.9	26.1	24.6	23.5	22.7	22.1	21.7	21.4
6.0	667	413	360	25.5	23.9	22.6	21.6	20.8	20.3	19.9	19.6
6.5	723	449	390	23.6	22.0	20.9	19.9	19.2	18.7	18.3	18.1
7.0	778	484	420	21.9	20.5	19.4	18.5	17.8	17.4	17.0	16.8
8.0	890	553	480	19.2	17.9	16.9	16.2	15.6	15.2	14.9	14.7
9.0	1001	622	540	17.0	15.9	15.1	14.4	13.9	13.5	13.2	13.1
10.0	1112	691	600	15.3	14.3	13.6	13.0	12.5	12.2	11.9	11.8

(To convert knots to other measures of speed, see Table 35.)

TABLE 40

GRADIENT WIND

The equation for the gradient wind speed V in cgs units is,

$$V = \frac{rf}{2}\left(-1 + \sqrt{1 + \frac{4V_g}{rf}}\right), \tag{1}$$

where

r = "radius of curvature" of the trajectory = R tan a (see Table 166),
f = Coriolis parameter $2\omega \sin \phi$ (ω = angular velocity of rotation of the earth, ϕ = latitude),
V_g = geostrophic wind speed (see Tables 37-39).

Equation (1) can be rewritten in the following form

$$V = \frac{3600\, rf}{2}\left(-1 + \sqrt{1 + \frac{4V_g}{3600\, rf}}\right) \tag{2}$$

for any of the following consistent combinations of units:

a. V and V_g in miles per hour, r in statute miles,
b. " " " " knots, r in nautical miles,
c. " " " " kilometers per hour, r in kilometers.

V is a function of the parameter rf and of the geostrophic wind speed V_g only. In applying equations (1) and (2) the following sign convention is necessary: for cyclonic curvature $rf > 0$, for anticyclonic curvature $rf < 0$.

Table 40 A gives values of the parameter rf as a function of latitude, ϕ, and r. Table 40 B gives values of V for cyclonic curvature and Table 40 C for anticyclonic curvature as a function of the parameter rf and the geostrophic wind speed V_g.

To find the gradient wind speed at a given point:

1. Determine the latitude ϕ and the value r of the trajectory. (Table 166 indicates a method for finding r on a polar stereographic map projection; for other projections an estimate must be made.)
2. From Table 40 A find the parameter rf. (This parameter is linear in r so that values for other radii than those given may be readily determined from the table, e.g., if $r = 2300$, add the values for $r = 2000$ and $r = 300$.)
3. Determine the geostrophic wind speed V_g at the given point (see Tables 37-39). (V_g and r must be in one of the consistent combinations of units given above.)
4. Enter Table 40 B (cyclonic case) or Table 40 C (anticyclonic case) with the arguments rf and V_g. The corresponding tabular value is the gradient wind V in the same units as V_g.

(*continued*)

GRADIENT WIND

TABLE 40 A.—Values of the parameter $r/$

Radius of curvature r	Latitude 10°	15°	20°	25°	30°	35°	40°	45°	50°	55°	60°	65°	70°	75°	80°	85°	90°
100	0.002	0.004	0.005	0.006	0.007	0.008	0.009	0.010	0.011	0.012	0.013	0.013	0.014	0.014	0.014	0.015	0.015
200	.005	.008	.010	.012	.015	.017	.019	.021	.022	.024	.025	.026	.027	.028	.029	.029	.029
300	.008	.011	.015	.018	.022	.025	.028	.031	.034	.036	.038	.040	.041	.042	.043	.044	.044
400	.010	.015	.020	.025	.029	.033	.037	.041	.045	.048	.051	.053	.055	.056	.057	.058	.058
500	.013	.019	.025	.031	.036	.042	.047	.052	.056	.060	.063	.066	.069	.070	.072	.073	.073
600	0.015	0.023	0.030	0.037	0.044	0.050	0.056	0.062	0.067	0.072	0.076	0.079	0.082	0.085	0.086	0.087	0.088
700	.018	.026	.035	.043	.051	.059	.066	.072	.078	.084	.088	.093	.096	.099	.101	.102	.102
800	.020	.030	.040	.049	.058	.067	.075	.083	.089	.096	.101	.106	.110	.113	.115	.116	.117
900	.023	.034	.045	.055	.066	.075	.084	.093	.101	.108	.114	.119	.123	.127	.129	.131	.131
1000	.025	.038	.050	.062	.073	.084	.094	.103	.112	.119	.126	.132	.137	.141	.144	.145	.146
1100	0.028	0.042	0.055	0.068	0.080	0.092	0.103	0.113	0.123	0.131	0.139	0.145	0.151	0.155	0.158	0.160	0.160
1200	.030	.045	.060	.074	.088	.100	.112	.124	.134	.143	.152	.159	.164	.169	.172	.174	.175
1300	.033	.049	.065	.080	.095	.109	.122	.134	.145	.155	.164	.172	.178	.183	.187	.189	.190
1400	.035	.053	.070	.086	.102	.117	.131	.144	.156	.167	.177	.185	.192	.197	.201	.203	.204
1500	.038	.057	.075	.092	.109	.126	.141	.155	.168	.179	.189	.198	.206	.211	.215	.218	.219
1600	0.041	0.060	0.080	0.099	0.117	0.134	0.150	0.165	0.179	0.191	0.202	0.211	0.219	0.225	0.230	0.232	0.233
1700	.043	.064	.085	.105	.124	.142	.159	.175	.190	.203	.215	.225	.233	.239	.244	.247	.248
1800	.046	.068	.090	.111	.131	.151	.169	.186	.201	.215	.227	.238	.247	.254	.259	.262	.263
1900	.048	.072	.095	.117	.139	.159	.178	.196	.212	.227	.240	.251	.260	.268	.273	.276	.277
2000	.051	.075	.100	.123	.146	.167	.187	.206	.223	.239	.253	.264	.274	.282	.287	.291	.292
2500	0.063	0.094	0.125	0.154	0.182	0.209	0.234	0.258	0.279	0.299	0.316	0.330	0.343	0.352	0.359	0.363	0.365
3000	.076	.113	.150	.185	.219	.251	.281	.309	.335	.358	.379	.397	.411	.423	.431	.436	.438

(continued)

TABLE 40 B.—Cyclonic curvature

V_g \ rf	.002	.004	.006	.008	.01	.02	.03	.04	.05	.06	.07	.08	.09	.10	.11	.12	.13	.14	.15	.16	.17	.18	.19	.20	.30	.40	.50	.60
5	3	4	4	4	4	5	5	5	5	5	5	5	5	5	5	5	5	5	5	5	5	5	5	5	5	5	5	5
10	6	7	7	8	8	9	9	9	10	10	10	10	10	10	10	10	10	10	10	10	10	10	10	10	10	10	10	10
15	7	9	10	11	11	13	13	14	14	14	14	14	14	14	14	14	15	15	15	15	15	15	15	15	15	15	15	15
20	9	11	13	14	14	16	17	18	18	18	19	19	19	19	19	19	19	19	19	19	19	19	20	20	20	20	20	20
25	10	13	15	16	17	20	21	22	22	23	23	23	23	24	24	24	24	24	24	24	24	24	24	24	24	25	25	25
30	12	15	17	18	20	23	24	26	26	27	27	27	29	28	28	28	28	28	28	29	29	29	29	29	29	29	30	30
35	13	16	19	20	22	26	28	29	30	31	31	32	32	32	32	33	33	33	33	33	33	33	33	33	34	34	34	34
40	14	18	20	22	24	28	31	33	34	34	35	36	36	36	37	37	37	37	37	38	38	38	38	38	39	39	39	39
45	15	19	22	24	26	31	34	36	37	38	39	40	40	40	41	41	41	42	42	42	42	42	42	42	43	44	44	44
50	16	21	24	26	28	34	37	39	41	42	43	43	44	44	45	45	46	46	46	46	46	47	47	47	48	48	49	49
60	18	23	27	30	32	39	43	46	48	49	50	51	52	52	53	53	54	54	54	55	55	55	56	56	57	58	58	58
70	19	25	28	33	35	44	48	52	54	56	57	58	59	60	61	61	62	62	63	63	63	64	64	64	66	67	68	68
80	21	28	32	36	39	48	54	57	60	62	64	65	66	67	68	69	70	70	71	71	72	72	72	73	75	76	77	77
90	22	30	35	38	42	52	58	63	66	68	70	72	73	75	76	76	77	78	78	79	80	80	80	81	84	85	86	86
100	24	31	37	41	45	56	63	68	72	74	77	79	80	82	83	84	85	86	86	87	88	88	88	89	92	94	95	96
120	26	35	41	46	50	64	72	78	82	86	89	91	93	95	96	98	99	100	101	102	103	104	104	105	109	111	113	114
140	28	38	45	51	55	71	80	87	92	97	100	103	106	108	110	111	113	114	115	116	117	118	119	120	125	129	130	132
160	30	41	49	55	60	77	88	96	102	107	111	114	117	120	122	124	126	128	129	130	132	133	134	135	142	145	148	150
180	33	44	52	59	64	83	96	104	111	117	122	125	129	132	134	137	139	141	142	144	145	147	148	149	157	162	165	167
200	34	47	56	63	69	89	102	112	120	126	131	136	140	143	146	149	151	153	155	157	159	160	162	163	172	178	182	184
220	36	50	59	66	73	95	109	120	128	135	141	146	150	154	157	160	163	166	168	170	172	174	175	177	187	194	198	201
240	38	52	62	70	77	100	116	127	136	144	150	156	160	165	168	172	175	178	180	182	184	186	188	190	202	209	214	218
260	40	54	65	73	80	106	122	134	144	152	159	165	170	175	179	183	186	189	192	194	197	199	201	203	217	225	230	235
280	41	57	68	77	84	110	128	141	152	161	168	174	180	185	189	193	197	200	203	206	209	211	213	216	231	240	246	251
300	43	59	70	80	88	115	134	148	159	168	176	183	189	195	199	204	208	211	215	218	220	223	226	228	245	255	262	267
340	46	63	76	86	94	125	145	161	173	184	193	200	207	214	219	224	228	233	236	240	243	246	249	252	272	284	292	299
380	49	67	80	91	100	133	156	173	187	198	208	217	224	231	238	243	248	253	257	261	265	269	272	275	298	312	322	330
420	52	71	85	96	106	142	166	184	199	212	223	232	241	249	255	262	267	273	278	282	286	290	294	297	323	340	351	360
460	54	74	90	102	112	150	175	195	212	225	237	247	257	265	272	279	286	292	297	302	307	311	315	319	348	367	380	390
500	56	78	94	106	117	157	185	206	223	238	251	262	272	281	289	297	304	310	316	321	326	331	336	340	372	393	408	419

(*continued*)

TABLE 40 C.—Anticyclonic curvature

V_g	rf	.006	.007	.008	.009	.01	.02	.03	.04	.05	.06	.07	.08	.09	.10	.11	.12	.13	.14	.15	.16	.17	.18	.19	.20	.30	.40	.50	.60
5		8	7	6	6	6	5	5	5	5	5	5	5	5	5	5	5	5	5	5	5	5	5	5	5	5	5	5	5
10							12	11	11	11	10	10	10	10	10	10	10	10	10	10	10	10	10	10	10	10	10	10	10
15							21	18	17	16	16	16	16	16	16	16	16	16	16	15	15	15	15	15	15	15	15	15	15
20								26	24	23	22	22	22	21	21	21	21	21	21	21	21	21	21	21	21	20	20	20	20
25								39	32	30	29	28	28	27	27	27	27	26	26	26	26	26	26	26	26	26	25	25	25
30									43	38	36	35	34	34	33	33	32	32	32	32	32	32	32	31	31	31	31	30	30
35									60	48	44	42	41	40	39	39	38	38	38	38	37	37	37	37	37	36	36	36	36
40										60	53	50	48	47	46	45	45	44	44	44	43	43	43	43	42	42	41	41	41
45											64	59	56	54	53	52	51	50	50	50	49	49	49	48	48	47	46	46	46
50											79	69	64	62	60	59	58	57	56	56	55	55	55	54	54	52	52	52	51
60												98	85	80	76	74	72	71	70	69	68	67	67	66	66	63	63	62	62
70													120	102	95	91	88	86	84	83	82	81	80	79	79	75	74	73	72
80														144	120	111	106	102	100	98	96	95	94	92	92	87	85	84	83
90																138	128	122	117	114	112	110	108	107	105	99	96	95	94
100																	157	145	138	132	129	126	124	122	120	112	108	106	105
120																			197	180	170	164	159	155	152	138	132	129	128
140																					240	217	205	196	190	165	157	153	151
160																							288	255	240	195	183	178	174
180																										228	211	203	198
200																										265	240	229	223
220																										308	271	257	249
240																										360	304	285	275
260																										436	340	315	302
280																											381	347	331
300																											426	380	360
340																											550	455	423
380																												545	492
420																												668	571
460																													664
500																													786

NOTE.—The critical value of V in the anticyclonic case is defined as that value of V for which the radical in equation (2) is equal to zero.

Values of V are tabulated only when they are less than the critical value. For imaginary values of equation (2) no gradient wind can be specified; if such a condition existed, the wind would not flow along the isobars. At the critical value of V, the following apply:

$$V_{critical} = 2V_g$$

$$(rf)_{critical} = -\frac{V_g}{900}$$

TABLE 166

RADIUS OF CURVATURE ON A POLAR STEREOGRAPHIC PROJECTION

In computing gradient wind speeds (Table 40) and in other problems it is necessary to determine a factor r which depends on curvature of the trajectory. This factor arises in taking account of the horizontal component of the centrifugal force acting on a particle. The problem is twofold: (1) to determine the trajectory of the particle on a map, and (2) to determine the required value of r if the trajectory on the map is known. The first problem is of such nature that it cannot be treated adequately here. (NOTE.—In many cases an approximation is made from the curvature of the isobars or streamlines.) The second problem has been solved for the case of a polar stereographic projection, since on this projection a "small circle" on the earth projects as a circle on the map. Table 40 provides a means for computing the desired r for trajectories on a polar stereographic projection.

Let R be the radius of the earth, r' the true radius of the "small circle" on which the particle is assumed to be traveling at a given instant, and a its angular radius (as seen from the center of the earth). Then $r' = R \sin a$. Since we are concerned with the horizontal component of the centrifugal force, the effective horizontal radius of the curvature required in the gradient wind equation is given by $r = r' \sec a = R \tan a$. If an arc on a map representing the instantaneous trajectory of a particle of air is determined, this arc may be regarded as a portion of a "small circle."

To determine r for a given arc of a trajectory on the map:

1. Complete the circle by extending the arc (a set of circular templates will prove very useful).
2. Find the meridian which passes through the center of this circle.
3. Determine the latitudes ϕ_1 and ϕ_2 of the points where this meridian intersects the circle (extend the meridian across the pole if necessary).

4A. If the circle found in step 1 *does not* contain the pole, find the difference between ϕ_1 and ϕ_2 and enter part A of the table with this difference as the argument. The corresponding tabular value is the required radius r in statute miles, from the formula $r = R \tan \frac{1}{2}(\phi_1 - \phi_2)$.

4B. If the circle found in step 1 contains the pole, find the sum $(\phi_1 + \phi_2)$ and enter part B of the table with this sum as the argument. The corresponding tabular value is the required radius r in statute miles, from the formula $r = R \tan [90° - \frac{1}{2}(\phi_1 + \phi_2)]$.

(continued)

TABLE 166

RADIUS OF CURVATURE ON A POLAR STEREOGRAPHIC PROJECTION

A. Circle not including pole.

$\phi_1 - \phi_0$	0	1	2	3	4	5	6	7	8	9
	mi.	mi.	mi.	mi.	mi.	mi.	mi.	mi.	mi.	mi.
0°	0	35	69	104	138	173	207	242	277	311
10	346	381	416	451	486	521	556	591	627	662
20	698	733	769	805	841	877	914	950	987	1023
30	1060	1097	1135	1172	1210	1248	1286	1324	1363	1401
40	1440	1479	1519	1559	1599	1639	1680	1721	1762	1803
50	1845	1887	1930	1973	2016	2060	2104	2148	2193	2239
60	2285	2331	2378	2425	2473	2521	2570	2619	2669	2720
70	2771	2822	2875	2928	2982	3036	3092	3148	3204	3262
80	3320	3380	3440	3501	3563	3626	3690	3755	3821	3889
90	3957									

B. Circle including pole.

$\phi_1 + \phi_0$	0	1	2	3	4	5	6	7	8	9
	mi.	mi.	mi.	mi.	mi.	mi.	mi.	mi.	mi.	mi.
0°		453433	226697	151110	113313	90631	75504	64697	56589	50278
10	45229	41093	37648	34730	32227	30057	28156	26477	24984	23646
20	22441	21350	20357	19449	18616	17849	17140	16482	15871	15301
30	14768	14269	13800	13358	12943	12550	12178	11825	11492	11174
40	10872	10583	10308	10045	9794	9553	9322	9100	8887	8683
50	8486	8296	8113	7937	7766	7601	7442	7288	7138	6994
60	6854	6718	6586	6457	6332	6211	6093	5978	5867	5757
70	5651	5547	5446	5347	5251	5157	5063	4973	4886	4800
80	4716	4633	4552	4473	4395	4318	4243	4170	4097	4027
90	3957	3889	3821	3755	3690	3626	3563	3501	3440	3380
100	3320	3262	3204	3148	3092	3036	2982	2928	2875	2822
110	2771	2720	2669	2619	2570	2521	2473	2425	2378	2331
120	2285	2239	2193	2148	2104	2060	2016	1973	1930	1887
130	1845	1803	1762	1721	1680	1639	1599	1559	1519	1479
140	1440	1401	1363	1324	1286	1248	1210	1172	1135	1097
150	1060	1023	987	950	914	877	841	805	769	733
160	698	662	627	591	556	521	486	451	416	381
170	346	311	277	242	207	173	138	104	69	35

DISTRIBUTION LIST FOR PUBLIC RELEASE

Commandant
U.S. Army Chemical School
ATTN: ATZN-CM-CC (S. Barnes)
Fort McClellan, AL 36205-5020

NASA/Marshall Space Flight Center
Deputy Director
Space Science Laboratory
Atmospheric Sciences Division
ATTN: ES01 (Dr. George H. Fichtl)
Huntsville, AL 35812

NASA/Marshall Space Center
ATTN: Code ES44 (Dale Johnson)
Huntsville, AL 35812

NASA/Marshall Space Flight Center
Atmospheric Sciences Division
ATTN: Code ED-41
Huntsville, AL 35812

Deputy Commander
U.S. Army Strategic Defense Command
ATTN: CSSD-SL-L
Dr. Julius Q. Lilly
P.O. Box 1500
Huntsville, AL 35807-3801

Commander
U.S. Army Missile Command
ATTN: AMSMI-RD-AC-AD
Donald R. Peterson
Redstone Arsenal, AL 35898-5242

Commander
U.S. Army Missile Command
ATTN: AMSMI-RD-AS-SS
Huey F. Anderson
Redstone Arsenal, AL 35898-5253

Commander
U.S. Army Missile Command
ATTN: AMSMI-RD-AS-SS
B. Williams
Redstone Arsenal, AL 35898-5253

Commander
U.S. Army Missile Command
ATTN: AMSMI-RD-DE-SE
Gordon Lill, Jr.
Redstone Arsenal, AL 35898-5245

Commander
U.S. Army Missile Command
Redstone Scientific Information Center
ATTN: AMSMI-RD-CS-R/Documents
Redstone, Arsenal, AL 35898-5241

Commander
U.S Army Intelligence Center and Fort Huachuca
ATTN: ATSI-CDC-C (Mr. Colanto)
Fort Huachuca, AZ 85613-7000

Northrup Corporation
Electronics Systems Division
ATTN: Dr. Richard D. Tooley
2301 West 120th Street, Box 5032
Hawthorne, CA 90251-5032

Commander - Code 3331
Naval Weapons Center
ATTN: Dr. Alexis Shlanta
China Lake, CA 93555

Commander
Pacific Missile Test Center
Geophysics Division
ATTN: Code 3250 (Terry E. Battalino)
Point Mugu, CA 93042-5000

Lockheed Missiles & Space Co., Inc.
Kenneth R. Hardy
Org/91-01 B/255
3251 Hanover Street
Palo Alto, CA 94304-1191

Commander
Naval Ocean Systems Center
ATTN: Code 54 (Dr. Juergen Richter)
San Diego, CA 92152-5000

Meteorologist in Charge
Kwajalein Missile Range
P.O. Box 67
APO San Francisco, CA 96555

U.S. Department of Commerce
Mountain Administration Support
Center
Library, R-51 Technical Reports
325 S. Broadway
Boulder, CO 80303

Dr. Hans J. Liebe
NTIA/ITS S 3
325 S. Broadway
Boulder, CO 80303

NCAR Library Serials
National Center for Atmos Rsch
P.O. Box 3000
Boulder, CO 80307-3000

HQDA
ATTN: DAMI-POI
Washington, DC 20310-1067

Mil Asst for Env Sci Ofc of
The Undersecretary of Defense
for Rsch & Engr/R&AT/E&LS
Pentagon - Room 3D129
Washington, DC 20301-3080

HQDA
DEAN-RMD/Dr. Gomez
Washington, DC 20314

Director
Division of Atmospheric Science
National Science Foundation
ATTN: Dr. Eugene W. Bierly
1800 G. Street, N.W.
Washington, DC 20550

Commander
Space & Naval Warfare System Command
ATTN: PMW-145-1G (LT Painter)
Washington, DC 20362-5100

Commandant
U.S. Army Infantry
ATTN: ATSH-CD-CS-OR
Dr. E. Dutoit
Fort Benning, GA 30905-5090

USAFETAC/DNE
Scott AFB, IL 62225

Air Weather Service
Technical Library - FL4414
Scott AFB, IL 62225-5458

USAFETAC/DNE
ATTN: Mr. Charles Glauber
Scott AFB, IL 62225-5008

Commander
U.S. Army Combined Arms Combat
ATTN: ATZL-CAW (LTC A. Kyle)
Fort Leavenworth, KS 66027-5300

Commander
U.S. Army Space Institute
ATTN: ATZI-SI (Maj Koepsell)
Fort Leavenworth, KS 66027-5300

Commander
U.S. Army Space Institute
ATTN: ATZL-SI-D
Fort Leavenworth, KS 66027-7300

Commander
Phillips Lab
ATTN: PL/LYP (Mr. Chisholm)
Hanscom AFB, MA 01731-5000

Director
Atmospheric Sciences Division
Geophysics Directorate
Phillips Lab
ATTN: Dr. Robert A. McClatchey
Hanscom AFB, MA 01731-5000

Raytheon Company
Dr. Charles M. Sonnenschein
Equipment Division
528 Boston Post Road
Sudbury, MA 01776
Mail Stop 1K9

Director
U.S. Army Materiel Systems
Analysis Activity
ATTN: AMXSY-MP (H. Cohen)
APG, MD 21005-5071

Commander
U.S. Army Chemical Rsch,
Dev & Engr Center
ATTN: SMCCR-OPA (Ronald Pennsyle)
APG, MD 21010-5423

Commander
U.S. Army Chemical Rsch,
Dev & Engr Center
ATTN: SMCCR-RS (Mr. Joseph Vervier)
APG, MD 21010-5423

Commander
U.S. Army Chemical Rsch,
Dev & Engr Center
ATTN: SMCCR-MUC (Mr. A. Van De Wal)
APG, MD 21010-5423

Director
U.S. Army Materiel Systems
Analysis Activity
ATTN: AMXSY-AT (Mr. Fred Campbell)
APG, MD 21005-5071

Director
U.S. Army Materiel Systems
Analysis Activity
ATTN: AMXSY-CR (Robert N. Marchetti)
APG, MD 21005-5071

Director
U.S. Army Materiel Systems
Analysis Activity
ATTN: AMXSY-CS (Mr. Brad W. Bradley)
APG, MD 21005-5071

Director
U.S. Army Research Laboratory
ATTN: AMSRL-D
2800 Powder Mill Road
Adelphi, MD 20783

Director
U.S. Army Research Laboratory
ATTN: AMSRL-OP-CI-A
(Technical Publishing)
2800 Powder Mill Road
Adelphi, MD 20783

Director
U.S. Army Research Laboratory
ATTN: AMSRL-OP-CI-AD, Record Copy
2800 Powder Mill Road
Adelphi, MD 20783

Director
U.S. Army Research Laboratory
ATTN: AMSRL-SS-SH
Dr. Z.G. Sztankay
2800 Powder Mill Road
Adelphi, MD 20783

National Security Agency
ATTN: W21 (Dr. Longbothum)
9800 Savage Road
Ft George G. Meade, MD 20755-6000

U. S. Army Space Technology
and Research Office
ATTN: Brenda Brathwaite
5321 Riggs Road
Gaithersburg, MD 20882

OIC-NAVSWC
Technical Library (Code E-232)
Silver Springs, MD 20903-5000

The Environmental Research
Institute of Michigan
ATTN: IRIA Library
P.O. Box 134001
Ann Arbor, MI 48113-4001

Commander
U.S. Army Research Office
ATTN: DRXRO-GS (Dr. W.A. Flood)
P.O. Box 12211
Research Triangle Park, NC 27709

Dr. Jerry Davis
North Carolina State University
Department of Marine, Earth, &
Atmospheric Sciences
P.O. Box 8208
Raleigh, NC 27650-8208

Commander
U. S. Army CECRL
ATTN: CECRL-RG (Dr. H. S. Boyne)
Hanover, NH 03755-1290

Commanding Officer
U.S. Army ARDEC
ATTN: SMCAR-IMI-I, Bldg 59
Dover, NJ 07806-5000

U.S. Army Communications-Electronics
Command EW/RSTA Directorate
ATTN: AMSEL-RD-EW-OP
Fort Monmouth, NJ 07703-5206

Commander
U.S. Army Satellite Comm Agency
ATTN: DRCPM-SC-3
Fort Monmouth, NJ 07703-5303

6585th TG (AFSC)
ATTN: RX (CPT Stein)
Holloman AFB, NM 88330

Department of the Air Force
OL/A 2nd Weather Squadron (MAC)
Holloman AFB, NM 88330-5000

PL/WE
Kirtland AFB, NM 87118-6008

Director
U.S. Army TRADOC Analysis Command
ATTN: ATRC-WSS-R
White Sands Missile Range, NM 88002

USAF Rome Laboratory Technical
Library, FL2810 Corridor W, Site 262,
RL//SUL (DOCUMENTS LIBRARY)
26 Electronics Parkway, Bldg 106
Griffiss AFB, NY 13441-4514

AFMC/DOW
Wright-Patterson AFB, OH 0334-5000

Commandant
U.S. Army Field Artillery School
ATTN: ATSF-TSM-TA
Mr. Charles Taylor
Fort Sill, OK 73503-5600

Commander
Naval Air Development Center
ATTN: Al Salik (Code 5012)
Warminister, PA 18974

Commander
U.S. Army Dugway Proving Ground
ATTN: STEDP-MT-DA-M
Mr. Paul Carlson
Dugway, UT 84022

Commander
U.S. Army Dugway Proving Ground
ATTN: STEDP-MT-DA-L
Dugway, UT 84022

Commander
U.S. Army Dugway Proving Ground
ATTN: STEDP-MT-M (Mr. Bowers)
Dugway, UT 84022-5000

Defense Technical Information Center
ATTN: DTIC-FDAC (2)
Cameron Station
Alexandria, VA 22314

Commanding Officer
U.S. Army Foreign Science &
Technology Center
ATTN: CM
220 7th Street, NE
Charlottesville, VA 22901-5396

Naval Surface Weapons Center
Code G63
Dahlgren, VA 22448-5000

Commander
U.S. Army OEC
ATTN: CSTE-EFS
Park Center IV
4501 Ford Ave
Alexandria, VA 22302-1458

Commander and Director
U.S. Army Corps of Engineers
Engineer Topographics Laboratory
ATTN: ETL-GS-LB
Fort Belvoir, VA 22060

TAC/DOWP
Langley AFB, VA 23665-5524

U.S. Army Topo Engineering Center
ATTN: CETEC-ZC
Fort Belvoir, VA 22060-5546

Commander
Logistics Center
ATTN: ATCL-CE
Fort Lee, VA 23801-6000

Commander
USATRADOC
ATTN: ATCD-FA
Fort Monroe, VA 23651-5170

Science and Technology
101 Research Drive
Hampton, VA 23666-1340

Commander
U.S. Army Nuclear & Cml Agency
ATTN: MONA-ZB Bldg 2073
Springfield, VA 22150-3198